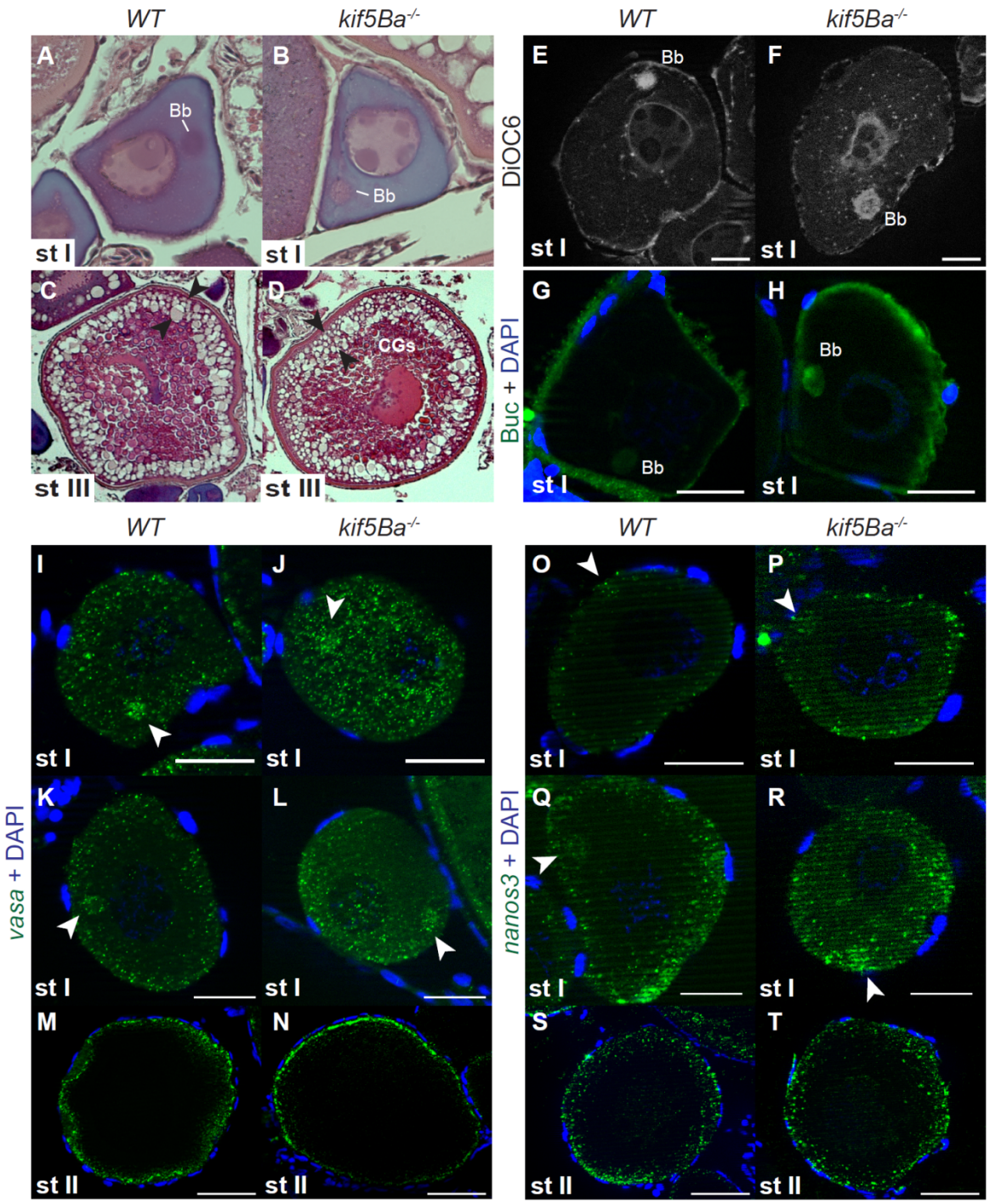

Figure S1. *kif5Ba* is dispensable for oocyte polarity and germ plasm localization.

(A-D) H&E staining of WT (A,C) and *kif5Ba*$^{-/-}$ mutant (B,D) oocytes showing polarized stage I (st I) oocytes with Balbiani bodies (Bb) and normal stage III (st III) oocytes with cortically-localized cortical granules (CGs, between arrowheads) and centrally localized

nucleus and yolk. (n=3 mutant ovaries analyzed, one each of *kif5Ba*$^{ae11/ae11}$, *kif5Ba*$^{ae11/ae12}$, and *kif5Ba*$^{ae12/ae12}$; assayed 5-10 oocytes for each genotype).

(E-F) DiOC6 staining reveals that ER and mitochondria are properly localized to the Bb in WT (E) and *kif5Ba*$^{-/-}$ mutant (F) st I oocytes. (n=18 oocytes analyzed from *kif5Ba*$^{ae11/ae11}$ mutant ovary, n=19 oocytes analyzed from WT ovary). Scale bars 20μm.

(G-H) Buc is properly localized to the Bb in WT (G) and *kif5Ba*$^{-/-}$ mutant (H) st I oocytes. (n=12 oocytes analyzed from *kif5Ba*$^{ae11/ae11}$ mutant ovary, n=10 oocytes analyzed from WT ovary)). Scale bars 20μm.

(I-T) *vasa* (I-N) and *nanos3* (O-T) RNA are enriched in the Bb (arrowheads) in early st I (I,J,O,P) and late st I (K,L,Q,R) oocytes in WT (I,K,O,Q) and *kif5Ba*$^{-/-}$ mutants (J,L,P,R). *vasa* RNA localizes to the cortex in WT (M) and *kif5Ba*$^{-/-}$ mutant (N) st II oocytes. *nanos3* RNA is diffuse throughout the cytosol of WT (S) and *kif5Ba*$^{-/-}$ mutant (T) st II oocytes. (n=3 WT and *kif5Ba*$^{ae12/ae12}$ mutant ovaries, assayed ≥10 oocytes for each condition). Scale bars 25μm (I-L, O-R), 25μm (M,N,S,T).

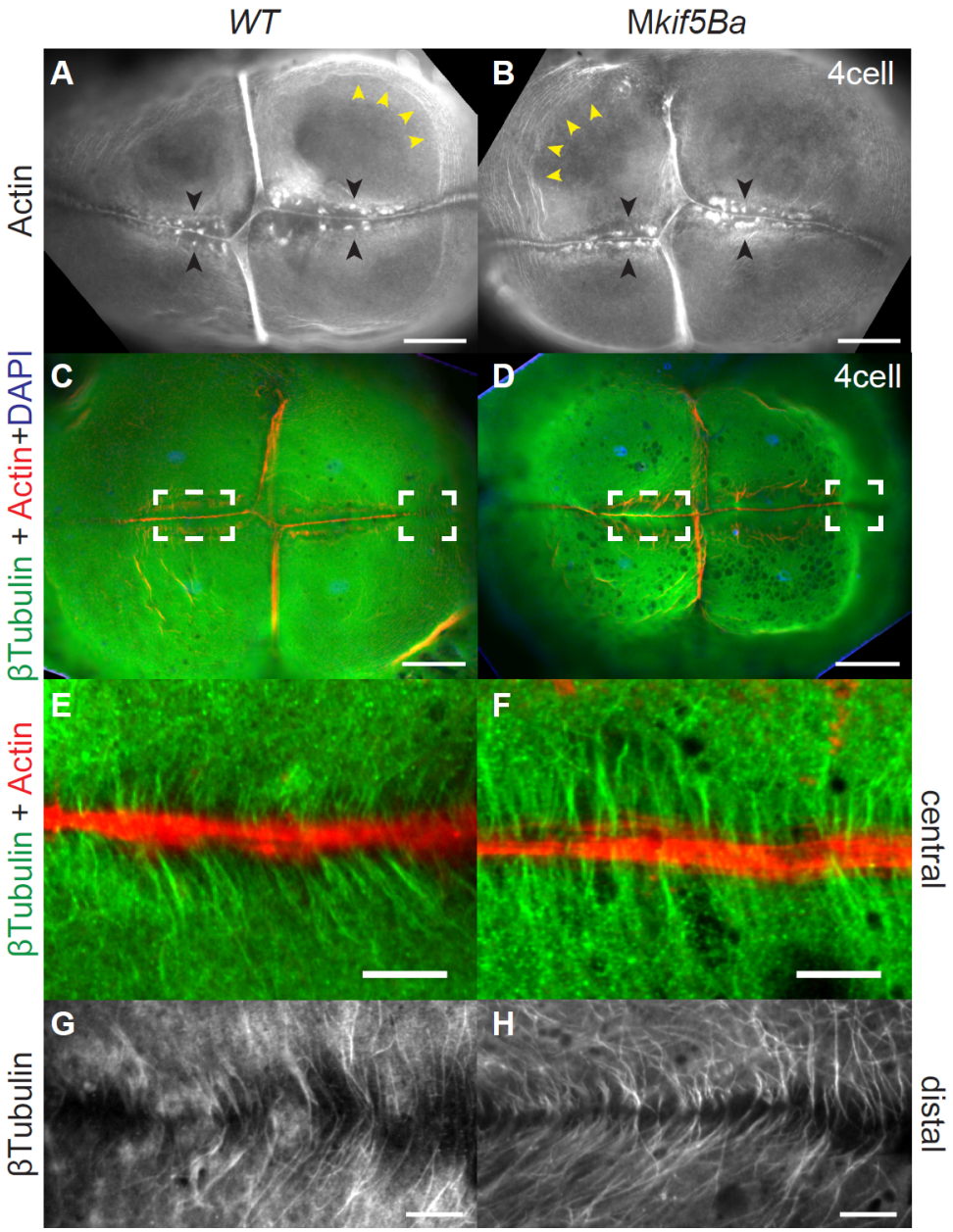

Figure S2. Cleavage furrow-associated cytoskeleton is intact in M*kif5Ba* mutants.

(A-B) Rhodamine-phalloidin staining to label F-actin. Animal pole views reveal an F-actin contractile band present in all four furrows, F-actin accumulations flanking the FMA (black arrowheads) and circumferential actin bands around the blastomeres (yellow arrowheads) in both WT (A) and Mkif5Ba mutants (B). Scale bars, 100μm.

(C-D) β-Tubulin antibody staining to reveal microtubules. Animal pole views show the F-actin contractile band present in all four furrows and the furrow microtubule arrays that flank the newly forming furrows of WT (C) and M*kif5Ba* mutants (D). Left and right dotted boxes in each panel indicate central and distal regions of the newly forming furrow respectively. Scale bars, 100μm.

(E-F) Higher magnification of the central furrow shows that the furrow microtubules are parallel to each other and perpendicular to the F-actin contractile band in both WT (E) and M*kif5Ba* mutants (F). Scale bars, 10μm.

(G-H) Higher magnification of the distal furrow shows microtubules angled in a V-shaped configuration pointing towards the distal end in both WT (G) and M*kif5Ba* mutants (H). Scale bars, 10μm. (All results are from n=11 embryos for M$kif5Ba^{ae11/ae12}$, n=9 for M$kif5Ba^{ae11/ae11}$, and n=15 for WT).

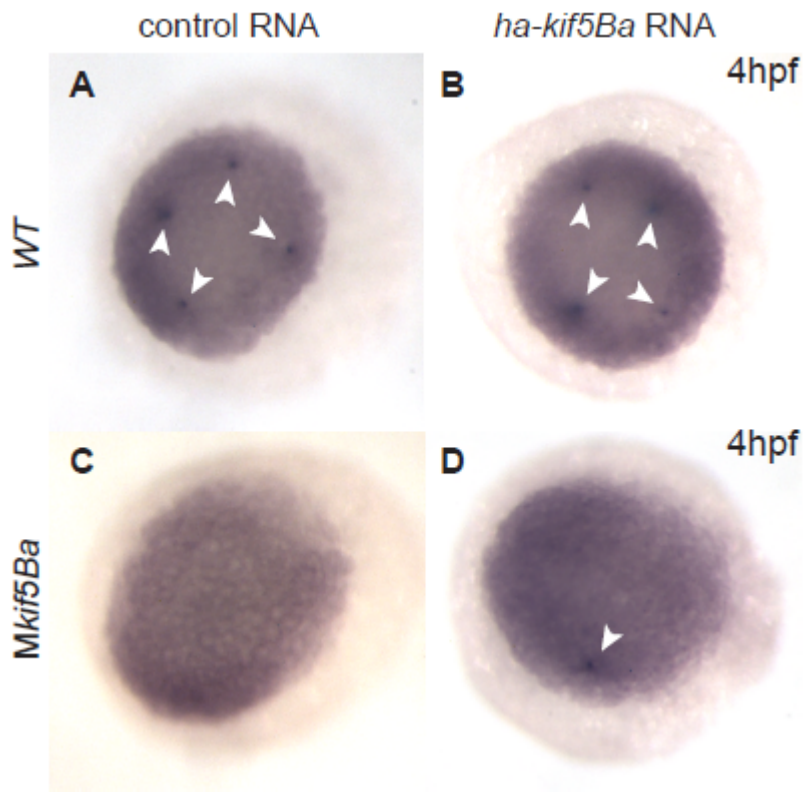

Figure S3. Injection of control RNA has no effect on number of PGCs in WT or M*kif5Ba* mutant embryos.

(A-B) The is no difference in the number of *nanos3*-positive PGCs at 4hpf in embryos injected with either 800pg of a control RNA encoding Cherry protein (A; 3.46±0.26 PGCs in n=37 embryos) or 800pg of *ha-kif5Ba* RNA (B; 3.56±0.25 PGCs in n=32 embryos)

(C-D) While injection of 800pg of a control RNA encoding Cherry protein has no effect on the number of PGCs in M*kif5Ba* mutants (C; zero PGCs in n=42/43 embryos, one PGC in n=1/43 embryos) injection of 800pg of *ha-kif5Ba* leads to the appearance of one PGC in a subset of M*kif5Ba* mutants (D; one PGC visible in 13/85 embryos). Compare with uninjected M*kif5Ba* mutants (zero PGCs in n=72/73 embryos, one PGC in n=1/73 embryos).

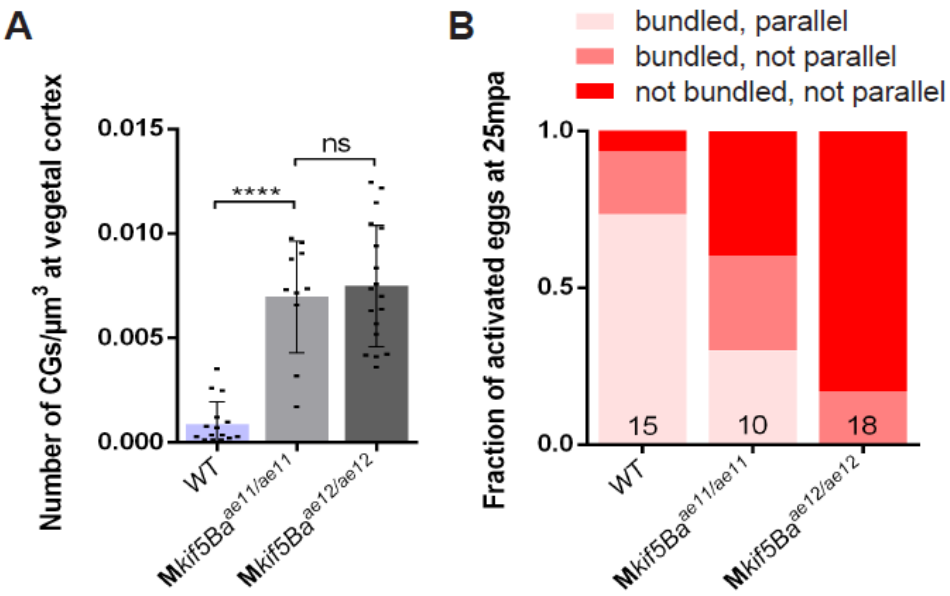

Figure S4. Severity of vegetal microtubule defect correlates with genotype and not degree of CG retention.

(A) There is no difference between the density of retained CGs at vegetal cortex at 25mpa in M*kif5Ba*$^{ae11/ae11}$ and M*kif5Ba*$^{ae12/ae12}$ mutants. Mean ± SD. One-way ANOVA, **** p<0.0001.

(B) The vegetal microtubules are more disorganized in M*kif5Ba*$^{ae12/ae12}$ compared to M*kif5Ba*$^{ae11/ae11}$ mutants.